Chemo-enzymatic synthesis of poly(4-piperidine lactone-b-#-pentadecalactone) block copolymers as biomaterials with antibacterial properties

Yan Xiao, Jinghao Pan, Dong Wang, Andreas Heise, and Meidong Lang

Biomacromolecules, **Just Accepted Manuscript** • DOI: 10.1021/acs.biomac.8b00296 • Publication Date (Web): 26 Apr 2018

Chemo-enzymatic synthesis of poly(4-piperidine lactone-*b*-*ω*-pentadecalactone) block copolymers as biomaterials with antibacterial properties

Yan Xiao[*1], *Jinghao Pan*[1], *Dong Wang*[1], *Andreas Heise*[2], *Meidong Lang*[*1]

1 Key Laboratory for Ultrafine Materials of Ministry of Education, School of Materials Science and Engineering, East China University of Science and Technology, Shanghai, 200237, China.

2 Department of Pharmaceutical and Medicinal Chemistry, Royal College of Surgeons in Ireland, St. Stephens Green, Dublin 2, Ireland.

Abstract: With increasing troubles in bacterial contamination and antibiotic-resistance, new materials possessing both biocompatibility and antimicrobial efficacy are supposed to be developed for future biomedical application. Herein, we demonstrated a chemo-enzymatic ring opening polymerization (ROP) approach for block copolyester, i.e., poly(4-benzyl formate piperidine lactone-*b*-ω-pentadecalactone) (PNPIL-*b*-PPDL), in a one-pot two-step process. Afterwards, cationic poly(4-piperidine lactone-*b*-ω-pentadecalactone) (PPIL-*b*-PPDL) with pendent secondary amino groups was obtained via acidic hydrolysis of PNPIL-*b*-PPDL. The resulting cationic block copolyester exhibited high antibacterial activity against Gram negative *E. coli* and Gram positive *S. aureus*, while showed low toxicity toward NIH-3T3 cells. Moreover, the antibacterial property, cytotoxicity and degradation behavior could be tuned

simply by variation of PPIL content. Therefore, we anticipate that such cationic block copolymers could potentially be applied as biomaterials for medicine or implants.

Keywords: PPDL; chemo-enzymatic; block copolymer; biocompatibility; antibacterial polyester

Introduction

In the past few decades, antibacterial materials have been developed for biomedical and healthcare applications ranging from wound treatment,[1-2] tissue regeneration,[3] bacterial colonization[4-5] and water purification.[6] Furnishing biologically inert polymers with functional entities is of high interest for the development of next generation biomedical polymers.[7] For example, methods have been employed to surface modify inert poly(ethylene), widely used in implants and hygiene products to impart antimicrobial properties.[8] However, chemical modification of poly(ethylene) or its incorporation into functional copolymer structures is tedious at best. A simple approach is the encapsulation of antimicrobial agents that show their biocidal activity by gradually releasing from the plastic.[9] But drug resistance[10] or decreased effectiveness may occur over time because of bacterial evolution and leaking of the loaded antimicrobial agent.[11] Antibiotics diffusion even causes environmental contamination and has a detrimental effect upon human health.[12-13] Cationic antimicrobial polymers with inherently antibacterial ability are therefore desirable as their efficacy derived from the component of the polymer itself, which provides a solution to overcome antibiotic-resistance and leakage of antibiotics.[14-15] Especially, polycations possess a selectivity between bacteria and mammalian cells thanks to much more abundant negative charges on membranes of bacteria than mammalian cells. However, most conventional antibacterial polymers usually possess non-degradable backbones that excludes them from certain biomedical applications.[16]

Polyesters from macrolactones offer an alternative. Especially, poly(ω-pentadecalactone) (PPDL) has been reported to have good biocompatibility with metabolic cells and excellent mechanical properties comparable to polyethylene.[17-18] Unlike low-density polyethylene, PPDL is linked with hydrolysable ester bonds. These ester units regularly placed along the backbone lead to potential use of PPDL as a biodegradable plastic and bioresorbable medical material.[19] The polymerization on pentadecalactone (PDL) as well as other macrolactones, by traditional ring-opening polymerization (ROP) catalysts is inefficient mainly due to the low ring strain of the monomers.[20-21] Therefore, many researchers have explored new catalysts for ROP of PDL including enzyme[22], organic and organometallic catalysts. It has been reported that a certain aluminum-salen complexes were remarkably efficient catalysts for the controlled ROP of macrolactones.[21, 23] When using organic catalysts like TBD, Bouyahyi and co-workers emphasized the difficulty in synthesis of PPDL-*b*-PCL block copolymers due to the rapid intra and intermolecular transesterification.[24] Enzymatic ROP of PDL has shown exceptionally high polymerization rate and afforded high molecular weight products.[25]

While PDL-based polymers have been applied, its high crystallinity, hydrophobicity and lack of functional groups mean it is hardly degradable and difficult to functionalize. However, it has been reported that by PDL copolymerization with other monomers it was possible to tune its properties towards compatibilizing agents[26], porous scaffold[27], gene carrier[28] and drug carrier[29] etc. Nonetheless, it remains challenging to achieve well-defined structures and variable functionality of PPDL materials required to expand the range of applications.

Our interest is in the introduction of antibacterial properties to PPDL, typically a property of cationic polymers. For instance, three series of pyridinium-methacrylate polymers differing in the spatial positioning of the positive charge and the pendant alkyl tail were synthesized via

radical polymerization of vinylpyridine (VP) and methyl methacrylate (MMA) followed by cationic modification with alkylating agent. The interplay between chemical structure and antibacterial vs hemolytic properties of these polymers were investigated in detail.[30] Qin *et al*. demonstrated a series of pyrrolidinium-type poly(ionic liquid) (PIL) polymers by reversible addition-fragmentation chain transfer (RAFT) polymerization of its small molecule IL with substitutions at the N position of pyrrolidinium cation. It was found that the antibacterial efficiency of PIL polymers increased with the increase of the alkyl chain length of substitution.[31] However, most pyridinium and pyrrolidinium functionalities were structurely complicated and their corresponding polymers were restricted to non-biodegradable acrylate backbones. Nederberg *et al*. revealed the first example of biodegradable quaternary ammonium-based polycarbonate nanoparticles synthesized by ROP of 3-chloropropyl 5-methyl-2-oxo-1,3-dioxane-5-carboxylate (MTC-$(CH_2)_3$Cl) and trimethylene carbonate (TMC). These cationic nanoparticles possessed excellent antibacterial even at a low concentration of 17.8 μg/mL.[32] Xiong and his coworkers have synthesized imidazolium cationic homo-polypeptide antimicrobials with a hydrophobic internal helical core and a charged exterior shell, which exhibited high antimicrobial activity and low hemolytic activity.[33] Engler *et al*. have developed a library of antibacterial polypeptides bearing cationic side groups including primary, secondary, tertiary, and quaternary amines on hydrocarbon side chains with different length. Furthermore, these polypeptides exhibited broad-spectrum antibacterial activity and low hemolytic activity. [34] Many factors affect antibacterial activity of polycations, including molecular weight, hydrophobicity, type of cationic charges.[35] Hedrick and co-workers developed a series of cationic polycarbonates with different lengths of alkyl chains between the quaternary ammonium moiety and the polymer backbone. With the spacer chain length increasing from 3 to 8, their MIC values against *E. coli*

decreased to 4 mg/L, which was lower than the natural peptide magainin-2 (MIC: 125 mg/L).[36-37] Cationic polymers can exhibit comparable antibacterial activity by manipulating the monomer components, which provided versatile methods to mitigate the toxicity, drug resistance and high manufacturing cost issues accompanying with small molecule drugs or antimicrobial peptides. However, most biodegradable cationic polymers were limited to polycarbonates and polypeptides, the design and antibacterial research of biodegradable cationic polyester has barely been reported.[38]

Herein, our previously reported 4-*N*-benzyl formate piperidinelactone (NPIL) monomer was copolymerized with PDL applying different catalytic systems. Novozym 435 (immobilized *Candida Antarctica* lipase B) and stannous 2-ethyl hexanoate ($Sn(Oct)_2$) were employed in copolymerization of PDL and NPIL by a "one-pot two-step" method. The resulting copolymer PNPIL-*b*-PPDL with a desired blocky structure was easily achieved by adding the monomers stepwise. It is worth noting that Novozym 435 preferred catalyzing ROP of PDL with larger ring size while $Sn(Oct)_2$ was prone to catalyze NPIL with smaller ring size. Subsequently, the protection group of PNPIL-*b*-PPDL copolymer was removed by the acidic hydrolysis to obtain cationic PPIL-*b*-PPDL with the secondary amine group anchoring on the backbone. For the potential application as an antibacterial biomaterial, the degradation behavior of PPIL-*b*-PPDL was investigated. More importantly, both antibacterial activity and low cytotoxicity were expected for these cationic block copolyesters.

Experimental Section

Materials.

Novozym 435 (immobilized *Candida Antarctica* lipase B, 10 000 PLU g^{-1}) was purchased from Novozymes A/S, Denmark and dried over P_2O_5 in a desiccator. Pentadecalactone (PDL)

(98%) was obtained from Alfa Aesar Chemical Co. Ltd and dried overnight on molecular sieves at ambient temperature. Triethylene glycol monomethy ether ($m(EG)_3$), stannous 2-ethyl hexanoate ($Sn(Oct)_2$) and *meta*-chloroperoxybenzoic acid (mCPBA) (85%) were purchased from Sigma-Aldrich. 4,4-Piperidinediol hydrochloride (98%) was bought from Shanghai Darui Finechemical Co. Ltd. Cellulose diacetate (CDA, M_w = 100 kDa) was purchased from Adamas reagent Co. Ltd. Toluene was dried by refluxing with sodium under argon. CH_2Cl_2 and ε-caprolactone (CL) were dried with CaH_2 for 24 h and freshly distilled before using. Gram-negative bacterium *Escherichia coli* (*E. coli*) (ATCC 25922) and Gram-positive bacterium *Staphylococus aureus* (*S. aureus*) (ATCC 25923) were purchased from Beijing Yuding Xinjie Technology Co. Ltd. The other reagents were purchased from Simopharm Chemical Reagent Co. Ltd (Shanghai, China) and used without further purification.

Methods.

All ^1H NMR (400 MHz) and ^{13}C NMR (125 MHz) spectra were recorded on a Bruker AV apparatus at 25 ^oC, using $CDCl_3$ or CF_3COOD as solvents. FTIR spectra was recorded on a Nicolet 5700 instrument at frequencies ranging from 500 to 4000 cm^{-1}. Samples were dissolved in chloroform and casted on a KBr pellet. The molecular weight and molecular weight distribution (PDI) of PPDL copolymers were determined by size exclusion chromatography (SEC) on Varian LC 1120 HPLC with $CDCl_3$ as eluent (flow rate: 1 mL min^{-1}; 35 ^oC) against polystyrene standard. Thermal analysis was carried out using a US Diamond differential scanning calorimeter (DSC) working with 5-10 mg samples in open aluminum pans. The samples were first heated from -100 to 150 ^oC at a heating rate of 20 ^oC min^{-1} and maintained at 150 ^oC for 5 min to eliminate the thermal history before quenching to -100 ^oC. Then the samples were reheated to 150 ^oC at a heating rate of 10 ^oC min^{-1}. Glass transition temperature (T_g) was

determined as the inflection point of the spectra in the second heating process. The water contact angles of copolyesters were determined by static contact angle measurements (Drop Shape Analyzer DSA100L, KRUESS, Germany). The morphologies of the porous films and bacterial were observed with SEM (S-3400N) and SEM (S-4800N), respectively. The samples were coated with gold under high vacuum and observed at 10-15 kV. Fluorescence microscopy images were taken by Leica DMI6000 B microscope.

Synthesis of 4-benzyl formate piperidine lactone (NPIL)

Potassium carbonate (69.1 g, 0.5 mol), 4,4-piperidinediol hydrochloride (20.4 g, 0.2 mol), deionized water (150 mL) and CH_2Cl_2 (80 mL) were added into a 500 mL flask with a magnetic bar. After the compounds were fully dissolved in an ice/water bath, benzyl chloroformate (32.7 mL, 0.33 mol) was dropwisely added with continuous stirring for 20 min. Then the reaction was heated to 60 ^oC with stirring for another 4 h. Afterwards, the mixture was extracted with CH_2Cl_2, washed with saturated sodium chloride for 3 times and dried with anhydrous magnesium sulfate ($MgSO_4$) overnight. The filtrate was evaporated and crude 4-benzyl formate piperidone was obtained. Baeyer-Villiger (BV) oxidation of 4-benzyl formate piperidone was then followed. 4-Benzyl formate piperidone (41.5 g, 0.18 mol) in CH_2Cl_2 (100 mL) was slowly added into a suspension of m-chloroperoxybenzoic acid (36.2 g, 0.18 mol) in 200 mL CH_2Cl_2 with a vigorously stirring in an ice/water bath. The reaction mixture was stirred for another 48 h in the ice/water bath. Then the solution was washed successively with saturated sodium thiosulfate solution (three times), bicarbonate solution (three times) and sodium chloride solution (three times). The organic extraction was dried with anhydrous $MgSO_4$, filtered and purified by column chromatography (silica gel, petroleum ether (PE): ethyl acetate (Et_2O) = 2:1) (yield: 72%).

Copolymerization of NPIL and PDL in one-pot, one step

Taking NPIL and PDL copolymerization as an example, NPIL (1.0 g, 4.0 mmol), PDL (0.96 g, 4.0 mmol) and $m(EG)_3$ (13.2 mg, 0.08 mmol) ([NPIL]/[PDL]/[$m(EG)_3$]=50:50:1) were added into a flame-dried Schlenk flask. Then, the mixture was heated to 40 ^oC under vigorous stirring for 3 h. Different catalysts of Novozym 435 (10 wt% of total monomers) or $Sn(Oct)_2$ (0.5 wt% of total monomers) in stock solution (20 μL) or their combination, as well as the toluene (8 mL) solvent were added into the flask, which was sealed under argon and immersed in an oil bath at 60 ^oC or 100 ^oC or (60 then 100 ^oC) for 24 h, respectively. The reaction was terminated by adding 4 mL cold chloroform and removing the enzyme by filtration. The filtrate was precipitated in cold anhydrous diethyl ether by centrifugation and dried under vacuum at room temperature. (yield: 40% (Novozym 435); 36% ($Sn(Oct)_2$); 82% (Novozym 435 and $Sn(Oct)_2$).

Copolymerization of NPIL and PDL in one-pot, two steps

NPIL (1.0 g, 4.0 mmol), PDL (0.96 g, 4.0 mmol) and $m(EG)_3$ (13.2 mg, 0.08 mmol) ([NPIL]/[PDL]/[$m(EG)_3$] =50:50:1 were added into a flame-dried Schlenk flask. Then the mixture was heated to 40 ^oC under vigorous stirring for 3 h. The $Sn(Oct)_2$ (0.5 wt% of NPIL) in stock solution (10 μL) was added into the flask via a microliter syringe. Then the flask was sealed under argon and heated to 120 ^oC for 24 h. After the reaction temperature cooling down to 60 ^oC, a mixture of Novozym 435 (10 wt% of PDL) and toulene (8 mL) were added into the flask under argon atmosphere. The reaction was continued in the oil bath at 60 ^oC for another 24 h and terminated by adding 4 ml cold chloroform and removing the enzyme by filtration. The filtrate was precipitated in cold anhydrous diethyl ether followed by centrifugation and dried under vacuum at room temperature. (yield: PDL 88%)

Deprotection of PNPIL-*b*-PPDL

Typically, $PNPIL_{50}$-*b*-$PPDL_{50}$ (0.8 g) in $CHCl_3$ (4 mL) was added into an argon-purged flame-dried Schlenk flask. After a quick addition 1.98 mL of HBr, the solution was slowly stirred in an ice/water bath for 20 min. Then the mixture was concentrated and precipitated in cold diethyl ether. The obtained product PPIL-*b*-PPDL was washed with diethyl ether for three times and dried at room temperature under vacuum. (yield: 92%)

Film preparation

Spin-coating was performed on circular coverslips (14 mm) which were cleaned by sonicating in ethanol for 15 min and acetone for another 15 min and dried under argon. 3% (w/v) solutions of cationic polymers in hexafluoroisopropanol (HFIP) and cellulose diacetate (CDA) in $CHCl_3$ were prepared respectively. The polymer solution was spin coated on the coverslips at 2000 rpm for 60 s then dried and annealed at 65 ^{o}C in a vacuum oven.

Degradation of PPIL-*b*-PPDL and PPDL polymers

A series of PPIL-*b*-PPDL copolymers and PPDL homopolymer were pressed into disk shape with a diameter of 8 mm using a hydraulic press. The *in vitro* degradation was carried out by immersing polymer disks in 10 mL of 5 mol/L NaOH in test tubes, which were kept in a shaking incubator at 37 ^{o}C. The disks were taken out at predetermined time intervals, rinsed with deionized water and dried in the oven. The mass of each disk was recorded before placing into a fresh NaOH solution.

Colony forming unit (CFU) counting method for antibacterial activities

Antibacterial activities of copolymer membranes were determined with a typical procedure.[39] The bacteria suspension ($1x10^5$ CFU/mL) was dropped onto the surfaces of polymer membranes coating on glass coverslips in the 12-well plates then incubated at 37^{o}C for 3 h. The blank coverslips without copolymers were set as control. Then inoculated copolymer films were

washed by 1 mL of PBS buffer and 100 μL of each dilution was spread on LB agar in a petri dish. The dishes were put into incubator at 37 °C for 24 h. The number of colonies was counted and all determinations were performed in triplicate to get an average value.

Morphological observation of the bacteria

0.1mL of bacteria suspension was dropped onto the polymer coated glass coverslips and incubated at 37 °C for 3 h. Then the coverslips were immersed in 2.5 wt % glutaraldehyde solution for 2 h at 4 °C. Then the obtained bacterial solution was gradiently eluted using 10%, 20%, 30%, 40%, 50%, 70%, 80%, 90% and 100% ethanol solution respectively and casted on the surface of a square silicon wafer (5 mm × 5 mm) followed by drying for 24 h at room temperature. Healthy bacteria without contacting with polymer films were set as control.

In Vitro Cytotoxicity

The toxicity of the cationic polymer membranes against NIH-3T3 mouse embryonic fibroblast cell was evaluated via 3-(4,5-dimethylthiazol-2-yl)-2,5-diphenyltetrazolium bromide (MTT) assay. Briefly, 3T3 cells were grown on sterilized glass coverslips coated with the polymers or a cellulose diacetate (CDA) control at ~5000 cells/cm^2. Cells were cultured in DMEM/ 10% fetal bovine serum (Hyclone) and 1% penicillin-streptomycin (10 000 U/mL, Thermo Fisher Scientific) at 37 °C in 5% CO_2 in a 24-well plate for 72 h. Then 100 μL of MTT solution (5 mg/mL in PBS) was added into each well. After another 4 h incubation at 37 °C, the MTT medium was removed meticulously. 750 μL of DMSO was added into each well to dissolve formazan crystals. The cell viability was measured by the absorbance of each sample at 490 nm (Bio Tek). All of the tests were performed in triplicate. The relative growth rate (RGR) of the 3T3 cells was calculated according to the following formula with CDA as control:

$$RGR = OD_{sample} / OD_{control} \times 100\%$$

In addition, live-dead staining for 3T3 cells was carried out to evaluate the cytotoxicity of polymer coatings as well. After seeding the cells onto the surface for 1 day and 3 days, Calcein AM and PI (Propidium iodide) were employed to stain the cells. A total of 250 μL each of 2 μM of calcein AM and 4.5 μM PI were added to each well. The stains were removed before the cells were incubated for 15-30 min, and the cells were imaged on the Leica DMI 6000 B microscope.

Results and discussion

Scheme 1. Synthetic route for ROP of NPIL and PDL in different catalytic systems.

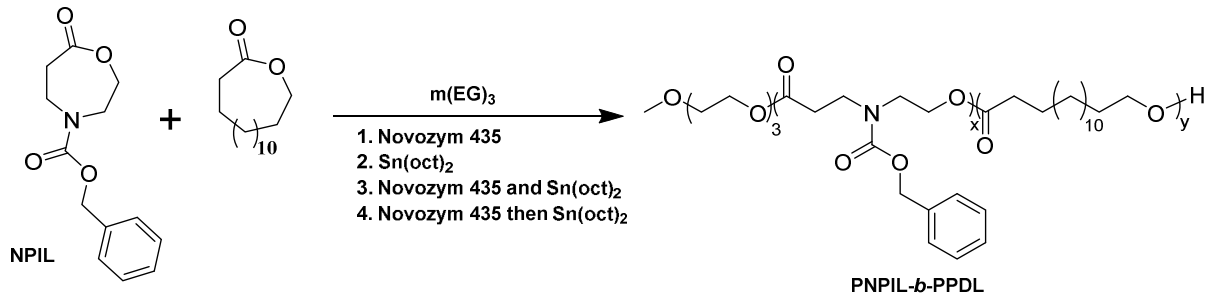

4-Benzyl formate piperidine lactone (NPIL) was synthesized by a two-step procedure including protection of a commercially available 4-piperidone hydrochloride with benzyl chloroformate followed by Baeyer-Villiger (BV) oxidation as previously reported by us (NMR spectra, Figure S1; EI-MS, Figure S2).[40] Copolymerization of NPIL and PDL was carried out in one pot using Novozym 435 or/and $Sn(Oct)_2$ as catalysts (Scheme 1). When Novozym 435 was added to the monomer mixture, almost exclusively PPDL homopolymer was obtained as evident from NMR analysis (Figure 1A). On the other hand, $Sn(Oct)_2$ only produced PNPIL homopolymer (Figure 1B). As summarized in Table 1 (Entries 1&2), a monomer feed ratio of 50/50 for PNPIL/PPDL, resulted in 3/48 or 48/4 ratio in the polymers, respectively. This selectivity is in agreement with the known catalytic activity of both catalysts. When both catalysts were present simultaneously, NMR analysis (Figure 1A (3)) revealed peaks for both

PPDL and PNPIL. In the ^{13}C NMR spectra of the homopolymers (Figure 1B (1&2)) the singlet peak at 174.1 ppm and the dual peaks at 171.3-171.6 ppm were attributed to the carbonyl groups of PPDL and PNPIL homopolymers, respectively. We carried out the synthetic procedure using two catalysts at 100°C at which two catalysts could keep active). A new peak appearing at 173.7 ppm was attributed to PDL carbonyl adjacent to NPIL repeat units, implying transesterification occurred. (Entry 3, Table 1.). Moreover, Figure S3 represents a unimodal SEC curve, which may exclude the presence of the mixture with two or more polymers. The calculated monomers incorporated in this copolymer (48/47) was very close to their feed ratio.

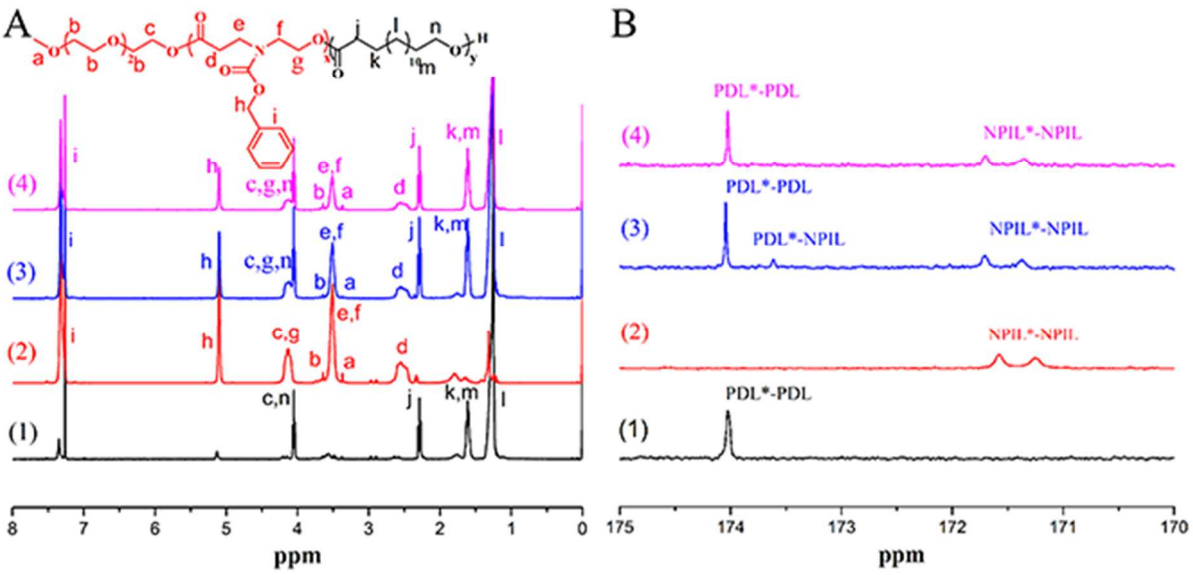

Figure 1. (A) ^{1}H NMR and (B) ^{13}C NMR spectra of products with catalytic systems of (1) Novozym 435; (2) $Sn(Oct)_2$; (3) Novozym 435 and $Sn(Oct)_2$; (4) $Sn(Oct)_2$ then Novozym 435.

Table. 1. Characterization of copolymerization of NPIL with PDL using Novozym 435 (N) and/or $Sn(Oct)_2$ (S).

Entry	Cat.	[NPIL]/ [PDL]^{a}	PNPIL-*b*-PPDL				
			[NPIL]/	M_n^{a}	M_n^{b}	M_n^{c}	Đ^{c}

			[PDL][b]	(g/mol)	(g/mol)	(g/mol)	
1	N	50/50	3/48	24600	13100	11000	1.31
2	S	50/50	48/4	24600	12400	8100	1.32
3	N and S	50/50	48/47	24600	23400	16100	1.45
4	S then N	50/50	48/48	24600	23600	17100	1.54

[a] Theoretical molecular weight (M_n) of polymers. $M_n = (M_{n\ NPIL} + M_{n\ PDL}) \times 50 + M_{n\ m(EG)3}$ [b] Calculated by ^{1}H NMR ($CDCl_3$) from the relative intensity of methylene ([M]) of NPIL at 2.6 ppm (-CH_2-, 2H), the methylene ([M]) of PDL at 2.4 ppm (-CH_2-, 2H), and the methyl signal ([I]) of m(EG)$_3$ at 3.3 ppm (-CH_3, 3H). $M_n = M_{n\ m(EG)3} + 3[M]/2[I]\ M_{n\ NPIL} + 3[M]/2[I]\ M_{n\ PDL}$ [c] Determined by SEC ($CHCl_3$ as eluent for each entry, PSt calibrants) Đ = polydispersity index.

Considering the above experiments, we hypothesized that ROP of NPIL catalyzed by Sn(Oct)$_2$ at high temperature could firstly yield PNPIL, which was then acted as a macro-initiator for ROP of PDL by N435 at 60 °C. With this one-pot/two-step procedure, relatively mild condition in the second step would minimize the possible transesterification so that a well-defined block copolymer was expected (as shown in Scheme 1 (4)). Entry 4 in Table 1 summarizes the results of this experiment. It was observed that DP of 48/48 for PNPIL/PPDL calculated by ^{1}H NMR was close to their feed ratio. Moreover, SEC curves (as shown in Figure S4) revealed unimodal peaks for PNPIL-*b*-PPDL and PNPIL macro-initiator. An obvious shift in retention time of PNPIL-*b*-PPDL compared with PNPIL before chain extension was observed, indicating an increase in molecular weight. To further verify the composition and block structure of the copolymer, PNPIL-*b*-PPDL was investigated by ^{13}C NMR (Figure 1B (4)). Quantitative ^{13}C NMR spectra of PPNIL$_{50}$-*b*-PPDL$_{50}$ (Figure S5) revealed only three resonances between 170 and 175 ppm corresponding to PPDL carbonyl (174 ppm) and PNPIL carbonyl (171.3-171.7ppm). The lack of other peaks within this region suggested that transesterification during reaction had been greatly suppressed. By the integration of the carbonyl peaks, the ratio of two monomers incorporated into copolymer were closed to 1:1. Additionally, the DOSY NMR spectrum (Figure S6) confirmed the copolymer structure of the PPDL and PNPIL in the absence of any

homopolymers (PNPIL or PPDL). Therefore, a block copolymer of NPIL and PDL was successfully synthesized by such one-pot/two-step procedure.

Synthesis and Characterization PPIL-*b*-PPDL Diblock Copolymers

Scheme 2. Synthesis route of PPIL-*b*-PPDL diblock copolymer.

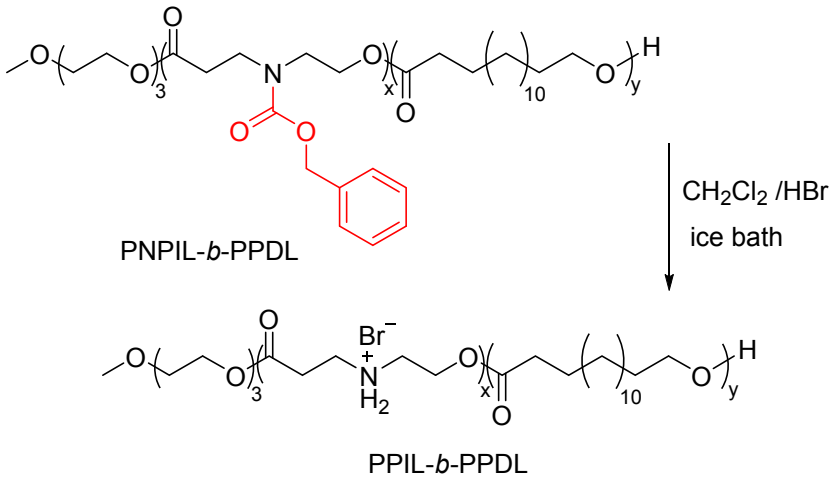

In the next step, synthesis of secondary amine functionalized block copolyesters was attempted by deprotection of the PNPIL-*b*-PPDL as illustrated in Scheme 2. According to our previous results[41], the protecting groups could be readily removed using HBr in CH_2Cl_2. ^{1}H NMR analysis in Figure 2A (IV) confirmed the disappearance of benzyl proton signals of the protecting groups at 5.09 ppm (j) and 7.30 ppm (i). Moreover, FTIR spectra of PPIL-*b*-PPDL in Figure 2B (b) also revealed the disappearance of characteristic peaks for protecting groups including C=O stretching vibration at 1703 cm^{-1} and the aromatic ring at 1471-1500 cm^{-1} and 700-730 cm^{-1}. With one-pot/two-step approach followed by deprotection, a series of (co)polyesters with various compositions of PPIL and PPDL were obtained as summarized in Table 2. Before deprotection, DPs of homopolymers and block copolymers determined by ^{1}H NMR were consistent with an overall targeted DP of 100. Thus PPDL-based blocky copolyesters with a variable ratio of secondary amine have been successfully prepared.

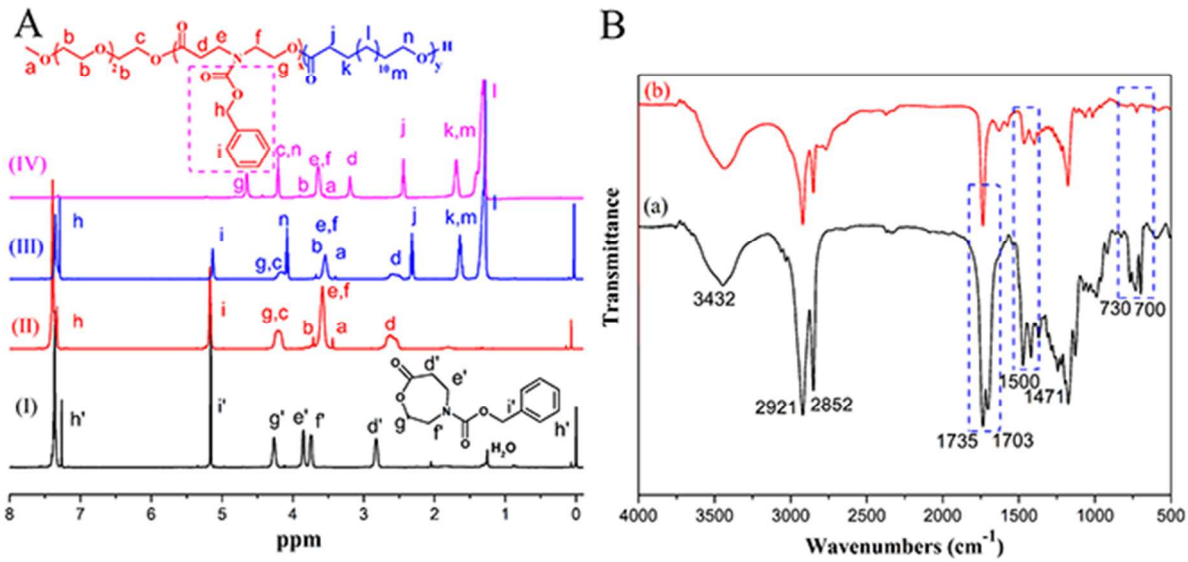

Figure 2 (A) ^{1}H NMR spectra of (I) NPIL, (II) PNPIL$_{50}$, (III) PNPIL$_{50}$-*b*-PPDL$_{50}$ and (IV) PPIL$_{50}$-*b*-PPDL$_{50}$. (B) FTIR spectra of (a) PNPIL$_{50}$-*b*-PPDL$_{50}$ and (b) PPIL$_{50}$-*b*-PPDL$_{50}$.

Table. 2. Molecular weight and thermal properties of prepared polymers before and after deprotection.

	n[NPIL]/[PDL]		PNPIL-*b*-PPDL							PPIL-*b*-PPDL					
Entry	In feed[a]	In polymer[b]	M_n[a] g/mol	M_n[b] g/mol	M_n[c] g/mol	Đ[c]	T (°C) T_{g1}	T_{g2}	T_m	In polymer[b]	M_n[a] g/mol	M_n[b] g/mol	T (°C) T_{g1}	T_{g2}	T_m
1	100/0	98/0	25100	24600	7900	1.29	—	-9.0	—	95/0	11700	10900	—	8.0	—
2	75/25	74/26	24800	24800	16700	1.50	-26.8	-9.5	94.3	72/24	14800	14000	-26.9	6.9	93.3
3	50/50	52/48	24600	24600	17200	1.58	-25.3	-9.3	95.5	49/47	17900	17300	-27.0	6.2	95.5
4	25/75	24/76	24400	24400	17800	1.55	-25.6	-9.7	96.8	23/75	21000	20800	-25.8	5.3	97.4
5	0/100	0/96	24200	23200	27200	1.52	-26.2	—	97.6	0/96	24200	23200	-26.2	—	97.6

[a] Theoretical molecular weight (M_n) of polymers. $M_n = M_{n\ m(EG)3} + DP_{NPIL} \times M_{n\ NPIL} + DP_{PDL} \times M_{n\ PDL}$ or $M_n = M_{n\ m(EG)3} + DP_{PIL} \times M_{n\ PIL} + DP_{PDL} \times M_{n\ PDL}$. [b] Calculated by ^{1}H NMR ($CDCl_3$) from the relative intensity of the methyl ([M]) of NPIL at 2.6 ppm (-CH_2-, 2H), the methylene ([M]) of PDL at 2.4 ppm (-CH_2-, 2H), the methylene ([M]) of PIL at 3.2 ppm (-CH_2-, 2H) and the methyl signal ([I]) of m(EG)$_3$ at 3.3 ppm (-CH_3, 3H). $M_n = M_{n\ m(EG)3} + 3[M]/2[I]\ M_{n\ NPIL} + 3[M]/2[I]\ M_{n\ PDL}$ or $Mn = M_{n\ m(EG)3} + 3[M]/2[I]\ M_{n\ PIL} + 3[M]/2[I]\ M_{n\ PDL}$. [c] Determined by SEC using $CHCl_3$ as eluent for PNPIL-*b*-PPDL.

Thermal analysis of the synthesized polymers was performed by DSC (Figure S7) and listed in Table 2. It was found that PNPIL homopolymer only displayed a glass transition temperature (T_g) at -9.0 ^oC, verifying its amorphous structure. Meanwhile, both T_g at -26.2 ^oC and the melting temperature (T_m) at 97.6 ^oC were observed for PPDL homopolymer, which is in agreement with what was reported by Gross et al.[42] In addition, it was found that P(N)PIL-*b*-PPDLs show two T_gs corresponding to each component, demonstrating their blocky distribution within the backbone. The melting temperature of block copolymers before and after de-protection of PNPIL slightly increased from 93.3 to 97.6 ^oC with increasing PDL content. It should be mentioned that T_g of PPIL was much higher than that of PNPIL, probably due to the hydrogen bonding between secondary amines after deprotection.[43] Moreover, the hydrophilicity of the copolymers was also greatly enhanced when higher PPIL composition was introduced as illustrated in Table S1.

Degradation behavior of PPDL and copolyesters

PPDL is considered as polyethylene-like material with high hydrophobicity and crystallinity, which explains the low susceptibility of PPDL to physiological degradation. Introduction of PPIL was expected to improve the biodegradability of the PPDL copolymer material for potentially biomedical application. Herein, accelerated degradation methods were used as a proof-of-concept to illustrate the degradation behavior of PPDL copolymers.[44] Four samples of PPIL-*b*-PPDL with DPs of 75/25, 50/50, 25/25 as well as PPDL 100 (denoted $PPIL_{75}$-*b*-$PPDL_{25}$, $PPIL_{50}$-*b*-$PPDL_{50}$, $PPIL_{25}$-*b*-$PPDL_{75}$ and $PPDL_{100}$**)** were pressed into disks and subjected to 5 M NaOH solutions at 37 ^oC. At predetermined intervals, the samples were weighed and the weight was plotted against degradation time as shown in Figure 3. As expected, degradation of $PPDL_{100}$ was the slowest with only a 12% mass loss achieved within 91 days, in accordance with the literature.[44] However, the three block copolymers of PPIL-*b*-PPDL were all completely degraded

within the experimental time scale. A three-stage degradation process was observed for all three copolymers. At stage I, the degradation of copolymers was relatively fast, corresponding to PPIL degradation because the weight loss agreed well with PPIL component in each copolymer. At stage II, the degradation rate dramatically slowed down because the remained highly crystalline PPDL was difficult to degrade. But the absence of PPIL components allowed water to gradually permeate the polymer disk during this stage. In stage III, the rate of degradation was significantly accelerated due to the decomposition of the PPDL blocks. The complete degradation of $PPIL_{75}$-*b*-$PPDL_{25}$, $PPIL_{50}$-*b*-$PPDL_{50}$ and $PPIL_{25}$-*b*-$PPDL_{75}$ disks took about 70, 84 and 91 days, respectively. As the degradation time was longer the higher the ratio of PPDL to PPIL in the copolymer, the desired degradation time could be manipulated by tuning the block copolymer ratio.

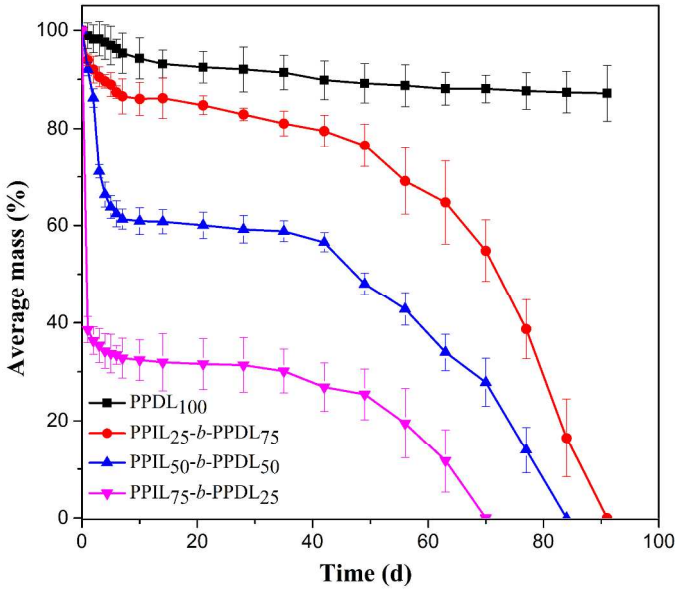

Figure 3. Average mass (%) of PPDL copolymer and homopolymer studied in accelerated degradation conditions (5 M NaOH, 37 ^{o}C).

Bactericidal Activity

Antibacterial properties are of essence for antibacterial materials. Colony forming units counting method was employed to determine contact-antibacterial activities. Bacterial cultures were dropped onto the copolyester membranes and incubated for 3 h. The antibacterial capacity could be evaluated based on the number of bacterial colonies on the agar plate (Figure S8). The calculated viability of *E. coli* and *S. aureus* are shown in Figure 4. Compared with the control, the PNPIL-b-PPDL copolymers with protected amine groups displayed no discernible difference in the viability of *E. coli* and *S. aureus* after contacting for 3 h. However, the survival of both bacteria decreased sharply with the increasing contents of PPIL. The results demonstrated that the antibacterial properties of the copolymer were derived from the cationic segments. Furthermore, $PPIL_{50}$-*b*-$PPDL_{50}$ and $PPIL_{75}$-*b*-$PPDL_{25}$ exhibited remarkable antibacterial activities against both *E. coli* and *S. aureus* (the relative bacterial viability was lower than 0.3%). Almost 100% bacteria on $PPIL_{75}$-*b*-$PPDL_{25}$ surface that processed highest cationic proportion were eliminated within 3 h contacting. Meanwhile, a paucity of antibacterial efficacy was observed in the $PPIL_{25}$-*b*-$PPDL_{75}$ entry which indicated that the ratio of the cationic fraction was a key contributor to the antibacterial property as well. Only cationic block copolymers bearing sufficient cationic composition could present significant antibacterial feature. An inhibition zone measurement was performed to investigate the non-leaching characteristic of the copolymers. As shown in Figure S9, after 24 h incubation on the agar plates, no visible inhibition zones formed in the area covered by polymer coatings. This substantiated the need for bacterial contact with the cationic surface to render antibacterial properties.

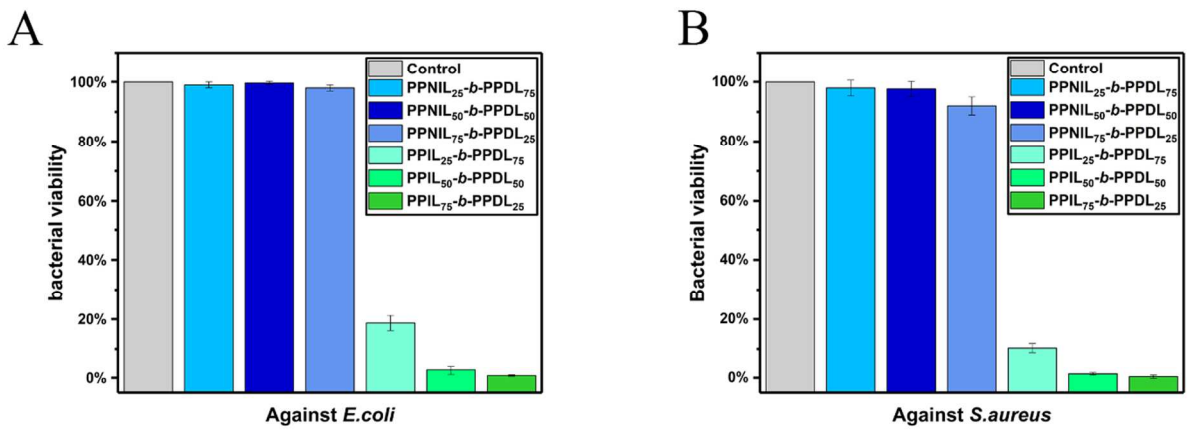

Figure 4. Bacterial viabilities of (A) *E. coli* and (B) *S. aureus* after 3 h contacting with PNPIL-*b*-PPDL and PPIL-*b*-PPDL copolymers.

We further investigated the morphology of bacteria after incubation with $PNPIL_{50}$-*b*-$PPDL_{50}$ and $PPIL_{50}$-*b*-$PPDL_{50}$ for 4 h by SEM. As indicated in Figure 5, *S. aureus* and *E. coli* seeded on the $PNPIL_{50}$-*b*-$PPDL_{50}$ membranes kept their smooth and intact surfaces as the healthy bacteria did. In contrast, collapsed and ruptured fusion bacterial surfaces were distinctly observed on the $PPIL_{50}$-*b*-$PPDL_{50}$ film surfaces, confirming that bacteria were killed by the deprotected copolymer. Additionally, *S. aureus* were found in broken state while *E. coli* were more likely to the dissolution of the inner solution (cytoplasm and ribosome), again suggesting distinct antibacterial mechanism when interacting with different bacteria.[45] It was therefore concluded that only those secondary amine functionalized copolyesters preserved antibacterial capability, which slightly differed with exposure to Gram negative bacterium *E. coli* and Gram positive bacterium *S. aureus*.

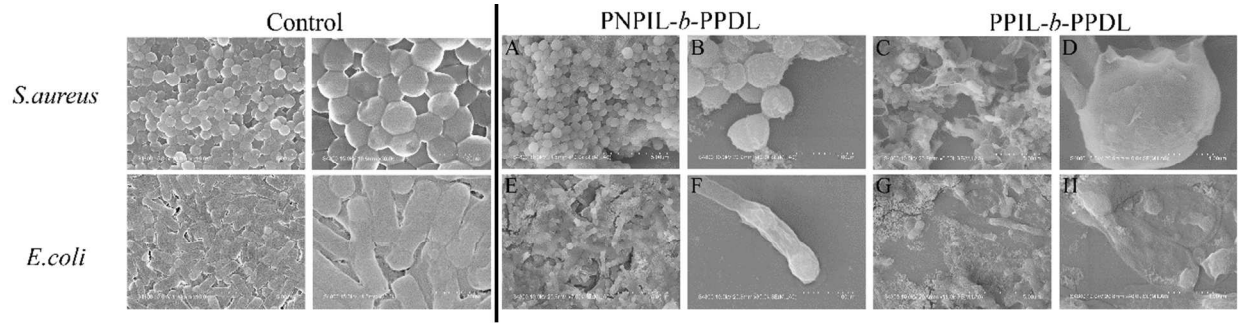

Figure 5. SEM images of *S. aureus* and *E. coil* cultured on block copolymers surfaces for 3 h. (left part: healthy bacterial morphologies, mid and right: B, D, F and H are expanded images of A, C, E and G, respectively).

Cytotoxicity Evaluation

Antibacterial materials with low cytotoxicity are preferably requested for their biomedical application. As shown in Figure 6, cytotoxicity of the cationic polymer membranes was evaluated by MTT assay. The NIH-3T3 cells were seeded on the surface of the block copolyester coatings with different PPIL contents. The relative growth rates (RGRs) of 3T3 cells were calculated according to the OD values at 490 nm from MTT assay. Compared to the well-known biocompatible CDA membranes, the RGRs values were 90.5%, 90.3% and 81.8% for $PPIL_{25}$-*b*-$PPDL_{75}$, $PPIL_{50}$-*b*-$PPDL_{50}$ and $PPIL_{75}$-*b*-$PPDL_{25}$, respectively. The values of RGR decreased slightly with increasing content of PPIL. It is worth noting that RGR value of 3T3 cells on $PPIL_{75}$-*b*-$PPDL_{25}$ films decreased to 81.8%, which could be ascribed to higher cationic contents leading to higher toxicity toward both mamanlian cells and bacteria. According to the standard toxicity rating, the toxicity grade with 80 % relative growth rate could be classified as grade 1, which indicated good biocompatibility.[46]

To visually elucidate the cytotoxicity, live-dead staining was performed to observe the viability of cells as shown in Figure 7. The cationic polymer coatings exhibited a negligible

cytotoxicity towards NIH-3T3 mouse embryonic fibroblast cells after 24 h or 72 h of culture. As abovementioned, cationic polymers have shown relatively high antimicrobial activity against *E. coli* and *S. aureus*. Therefore, this cationic block copolymer could discriminate between bacteria and 3T3 cells, possibly due to more negative charges on bacteria cells surface than mammalian cells.[36] Moreover, the NIH-3T3 cells were normally proliferated on the copolymer surfaces after 3 days incubation. The low toxicity could be ascribed to the excellent biocompatibility of PPDL[47] components that promote cell growth.

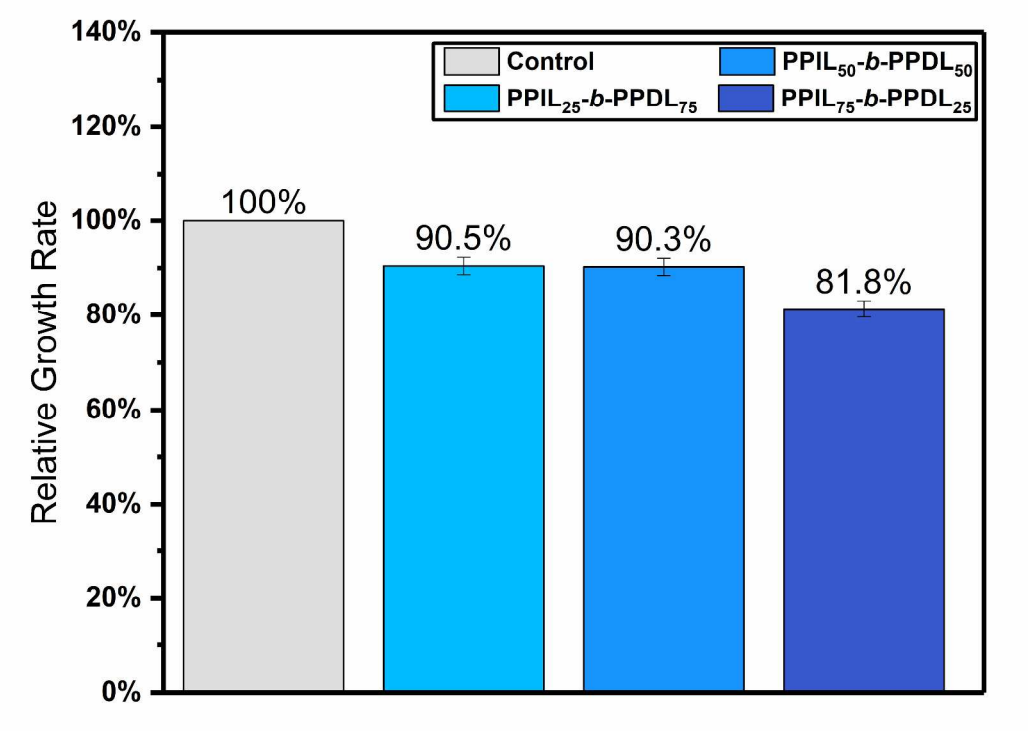

Figure 6. Relative growth rate (RGR) of various PPIL contents membranes to mouse embryonic fibroblast cells detected by MTT assay

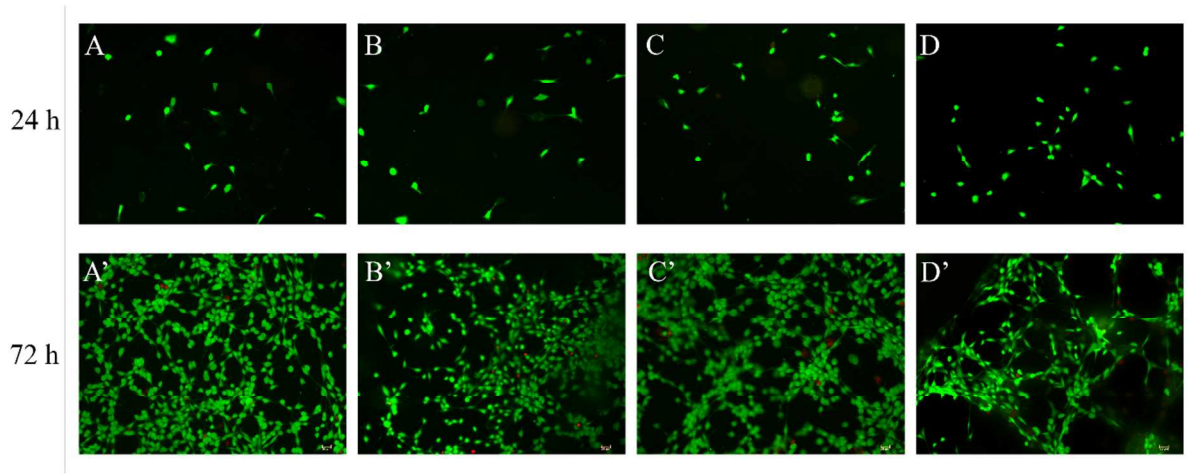

Figure 7. Fluorescence microscopy images (10× magnification) of NIH-3T3 mouse embryonic fibroblast cells after 24 h on CDA (A), $PPIL_{25}$-*b*-$PPDL_{75}$ (B), $PPIL_{50}$-*b*-$PPDL_{50}$ (C), $PPIL_{75}$-*b*-$PPDL_{25}$ (D) surfaces. After 72 h on CDA (A'), $PPIL_{25}$-*b*-$PPDL_{75}$ (B'), $PPIL_{50}$-*b*-$PPDL_{50}$ (C'), $PPIL_{75}$-*b*-$PPDL_{25}$ (D') surfaces after live-dead staining. Green indicates viable cells, and red indicates dead cells.

Conclusion

Based on control experiments, Novozym 435 and $Sn(Oct)_2$ were found highly complementary in catalyzing ROP of PDL and NPIL. Consequently, block copolyesters of PNPIL-*b*-PPDL were rationally designed and successfully synthesized via chemo-enzymatic approach in one-pot/two-step. The molecular weight and sequential structures of the resulted products were carefully evaluated by NMR and SEC. Furthermore, well-defined PPIL-*b*-PPDL copolymers bearing secondary amino groups were achieved via acidic hydrolysis of PNPIL-*b*-PPDL. The degradation of PPIL-*b*-PPDL copolymers could be greatly accelerated and well-tuned by the PPIL content. Moreover, PPIL-*b*-PPDL exhibited remarkably antibacterial activities against *E. coli* and S. *aureus* while showed no obviously deleterious effects on NIH-3T3 cells. Thus, a subtle balance between antibacterial property and biocompatibility could be achieved via tuning

PPIL contents in the copolymer. Therefore, the block copolyesters with well-defined structure, tunable biodegradability, biocompatibility and excellent antibacterial property would have great potential in biomedical application.

ASSOCIATED CONTENT

Supporting Information

Details of ^{1}H and ^{13}C NMR spectra, SEC traces, EI-MS data, DSC curves, contact angles data and antibacterial test images. This material is available free of charge via the Internet at http://pubs.acs.org.

AUTHOR INFORMATION

Corresponding Author

* *E-mail: yxiao@ecust.edu.cn*; *mdlang@ecust.edu.cn*

Notes

The authors declare no competing financial interest.

ACKNOWLEDGMENT

Y.X., J.P. and D.W. acknowledged financial supports from the National Natural Science Foundation of China (21674037) and the Shanghai Scientific and Technological Innovation Project (14520720600). M.L. acknowledged the National Key Research and Development Program (2016YFC1100703). A.H. acknowledged financial support from the Science Foundation Ireland (SFI) Principle Investigator Award 13/IA/1840..

REFERENCES

(1) Zhu, Y.; Zhang, J.; Song, J.; Yang, J.; Xu, T.; Pan, C.; Zhang, L. One-step synthesis of an antibacterial and pro-healing wound dressing that can treat wound infections. *J. Mater. Chem. B* **2017,** *5* (43), 8451-8458.
(2) Li, C.; Ye, R.; Bouckaert, J.; Zurutuza, A.; Drider, D.; Dumych, T.; Paryzhak, S.; Vovk, V.; Bilyy, R. O.; Melinte, S.; Li, M.; Boukherroub, R.; Szunerits, S. Flexible Nanoholey Patches for Antibiotic-Free Treatments of Skin Infections. *ACS Appl. Mater. Interfaces* **2017,** *9* (42), 36665-36674.
(3) Nasajpour, A.; Ansari, S.; Rinoldi, C.; Rad, A. S.; Aghaloo, T.; Shin, S. R.; Mishra, Y. K.; Adelung, R.; Swieszkowski, W.; Annabi, N.; Khademhosseini, A.; Moshaverinia, A.; Tamayol, A. A Multifunctional Polymeric Periodontal Membrane with Osteogenic and Antibacterial Characteristics. *Adv. Funct. Mater.* **2018,** *28* (3), 1703437-1703445.
(4) Wei, T.; Tang, Z.; Yu, Q.; Chen, H. Smart Antibacterial Surfaces with Switchable Bacteria-Killing and Bacteria-Releasing Capabilities. *ACS Appl. Mater. Interfaces* **2017,** *9* (43), 37511-37523.
(5) Keum, H.; Kim, J. Y.; Yu, B.; Yu, S. J.; Kim, J.; Jeon, H.; Lee, D. Y.; Im, S. G.; Jon, S. Prevention of Bacterial Colonization on Catheters by a One-Step Coating Process Involving an Antibiofouling Polymer in Water. *ACS Appl. Mater. Interfaces* **2017,** *9* (23), 19736-19745.
(6) Dankovich, T. A.; Smith, J. A. Incorporation of copper nanoparticles into paper for point-of-use water purification. *Water Research* **2014,** *63*, 245-251.
(7) Krishnamoorthy, M.; Hakobyan, S.; Ramstedt, M.; Gautrot, J. E. Surface-Initiated Polymer Brushes in the Biomedical Field: Applications in Membrane Science, Biosensing, Cell Culture, Regenerative Medicine and Antibacterial Coatings. *Chemical Reviews* **2014,** *114* (21), 10976-11026.
(8) Zapata, P. A.; Tamayo, L.; Páez, M.; Cerda, E.; Azócar, I.; Rabagliati, F. M. Nanocomposites based on polyethylene and nanosilver particles produced by metallocenic "in situ" polymerization: synthesis, characterization, and antimicrobial behavior. *Eur. Polym. J.* **2011,** *47* (8), 1541-1549.
(9) Marchetti, F.; Palmucci, J.; Pettinari, C.; Pettinari, R.; Marangoni, M.; Ferraro, S.; Giovannetti, R.; Scuri, S.; Grappasonni, I.; Cocchioni, M.; Maldonado Hodar, F. J.; Gunnella, R. Preparation of Polyethylene Composites Containing Silver(I) Acylpyrazolonato Additives and SAR Investigation of their Antibacterial Activity. *ACS Appl Mater Interfaces* **2016,** *8* (43), 29676-29687.
(10) Arias, C. A.; Murray, B. E. Antibiotic-Resistant Bugs in the 21st Century — A Clinical Super-Challenge. *N. Engl. J. Med.* **2009,** *360* (5), 439-443.
(11) Xue, Y.; Xiao, H.; Zhang, Y. Antimicrobial polymeric materials with quaternary ammonium and phosphonium salts. *Int J Mol Sci* **2015,** *16* (2), 3626-55.
(12) Fuchs, A. D.; Tiller, J. C. Contact-Active Antimicrobial Coatings Derived from Aqueous Suspensions. *Angew.Chem., Int. Ed.* **2006,** *45* (40), 6759-6762.
(13) Thomassin, J.-M.; Lenoir, S.; Riga, J.; Jérôme, R.; Detrembleur, C. Grafting of Poly[2-(tert-butylamino)ethyl methacrylate] onto Polypropylene by Reactive Blending and Antibacterial Activity of the Copolymer. *Biomacromolecules* **2007,** *8* (4), 1171-1177.
(14) Hook, A. L.; Chang, C.-Y.; Yang, J.; Luckett, J.; Cockayne, A.; Atkinson, S.; Mei, Y.; Bayston, R.; Irvine, D. J.; Langer, R.; Anderson, D. G.; Williams, P.; Davies, M. C.; Alexander, M. R. Combinatorial discovery of polymers resistant to bacterial attachment. *Nature Biotechnology* **2012,** *30*, 868-875.

(15) Majumdar, P.; Lee, E.; Gubbins, N.; Stafslien, S. J.; Daniels, J.; Thorson, C. J.; Chisholm, B. J. Synthesis and antimicrobial activity of quaternary ammonium-functionalized POSS (Q-POSS) and polysiloxane coatings containing Q-POSS. *Polymer* **2009,** *50* (5), 1124-1133.
(16) Sellenet, P. H.; Allison, B.; Applegate, B. M.; Youngblood, J. P. Synergistic Activity of Hydrophilic Modification in Antibiotic Polymers. *Biomacromolecules* **2007,** *8* (1), 19-23.
(17) Vaida, C.; Keul, H.; Moeller, M. Tailor-made polyesters based on pentadecalactonevia enzymatic catalysis. *Green Chem.* **2011,** *13* (4), 889-899.
(18) Wilson, J. A.; Hopkins, S. A.; Wright, P. M.; Dove, A. P. 'Immortal' ring-opening polymerization of ω-pentadecalactone by Mg(BHT)2(THF)2. *Polym. Chem.* **2014,** *5* (8), 2691-2694.
(19) Kalra, B.; Kumar, A.; Gross, R. A.; Baiardo, M.; Scandola, M. Chemoenzymatic Synthesis of New Brush Copolymers Comprising Poly(ω-pentadecalactone) with Unusual Thermal and Crystalline Properties. *Macromolecules* **2004,** *37* (4), 1243-1250.
(20) Pascual, A.; Leiza, J. R.; Mecerreyes, D. Acid catalyzed polymerization of macrolactones in bulk and aqueous miniemulsion: Ring opening vs. condensation. *Eur Polym J* **2013,** *49* (6), 1601-1609.
(21) Pepels, M. P. F.; Hofman, W. P.; Kleijnen, R.; Spoelstra, A. B.; Koning, C. E.; Goossens, H.; Duchateau, R. Block Copolymers of "PE-Like" Poly(pentadecalactone) and Poly(l-lactide): Synthesis, Properties, and Compatibilization of Polyethylene/Poly(l-lactide) Blends. *Macromolecules* **2015,** *48* (19), 6909-6921.
(22) Veld, M. A. J.; Palmans, A. R. A.; Meijer, E. W. Selective polymerization of functional monomers with Novozym 435. *Journal of Polymer Science Part A: Polymer Chemistry* **2007,** *45* (24), 5968-5978.
(23) Xu, Y. C.; Ren, W. M.; Zhou, H.; Gu, G. G.; Lu, X. B. Functionalized Polyesters with Tunable Degradability Prepared by Controlled Ring-Opening (Co)polymerization of Lactones. *Macromolecules* **2017,** *50* (8), 3131-3142.
(24) Bouyahyi, M.; Pepels, M. P. F.; Heise, A.; Duchateau, R. ω-Pentandecalactone Polymerization and ω-Pentadecalactone/ε-Caprolactone Copolymerization Reactions Using Organic Catalysts. *Macromolecules* **2012,** *45* (8), 3356-3366.
(25) And, G. C.; Scandola, M.; Kumar, A.; Bhanu Kalra, A.; Gross, R. A. Cocrystallization of Random Copolymers of ω-Pentadecalactone and ε-Caprolactone Synthesized by Lipase Catalysis. *Biomacromolecules* **2005,** *6* (2), 902-907.
(26) Todd, R.; Tempelaar, S.; Lo Re, G.; Spinella, S.; McCallum, S. A.; Gross, R. A.; Raquez, J.-M.; Dubois, P. Poly(ω-pentadecalactone)-b-poly(l-lactide) Block Copolymers via Organic-Catalyzed Ring Opening Polymerization and Potential Applications. *ACS Macro Lett.* **2015,** *4* (4), 408-411.
(27) Gualandi, C.; White, L. J.; Chen, L.; Gross, R. A.; Shakesheff, K. M.; Howdle, S. M.; Scandola, M. Scaffold for tissue engineering fabricated by non-isothermal supercritical carbon dioxide foaming of a highly crystalline polyester. *Acta Biomater.* **2010,** *6* (1), 130-136.
(28) Chen, Y.; Li, Y.; Gao, J.; Cao, Z.; Jiang, Q.; Liu, J.; Jiang, Z. Enzymatic PEGylated Poly(lactone-co-beta-amino ester) Nanoparticles as Biodegradable, Biocompatible and Stable Vectors for Gene Delivery. *ACS Appl Mater Interfaces* **2016,** *8* (1), 490-501.
(29) Liu, B.; Zhang, X.; Chen, Y.; Yao, Z.; Yang, Z.; Gao, D.; Jiang, Q.; Liu, J.; Jiang, Z. Enzymatic synthesis of poly([small omega]-pentadecalactone-co-butylene-co-3,3[prime or minute]-dithiodipropionate) copolyesters and self-assembly of the PEGylated copolymer

micelles as redox-responsive nanocarriers for doxorubicin delivery. *Polym. Chem.* **2015,** *6* (11), 1997-2010.
(30) Sambhy, V.; Peterson, B. R.; Sen, A. Antibacterial and Hemolytic Activities of Pyridinium Polymers as a Function of the Spatial Relationship between the Positive Charge and the Pendant Alkyl Tail. *Angew.Chem., Int. Ed.* **2008,** *47* (7), 1250-1254.
(31) Qin, J.; Guo, J.; Xu, Q.; Zheng, Z.; Mao, H.; Yan, F. Synthesis of Pyrrolidinium-Type Poly(ionic liquid) Membranes for Antibacterial Applications. *ACS Appl. Mater. Interfaces* **2017,** *9* (12), 10504-10511.
(32) Nederberg, F.; Zhang, Y.; Tan, J. P. K.; Xu, K.; Wang, H.; Yang, C.; Gao, S.; Guo, X. D.; Fukushima, K.; Li, L.; Hedrick, J. L.; Yang, Y.-Y. Biodegradable nanostructures with selective lysis of microbial membranes. *Nat. Chem.* **2011,** *3*, 409-414.
(33) Xiong, M.; Lee, M. W.; Mansbach, R. A.; Song, Z.; Bao, Y.; Peek, R. M.; Yao, C.; Chen, L.-F.; Ferguson, A. L.; Wong, G. C. L.; Cheng, J. Helical antimicrobial polypeptides with radial amphiphilicity. *Proc. Natl. Acad. Sci. U. S. A.* **2015,** *112* (43), 13155-13160.
(34) Engler, A. C.; Shukla, A.; Puranam, S.; Buss, H. G.; Jreige, N.; Hammond, P. T. Effects of Side Group Functionality and Molecular Weight on the Activity of Synthetic Antimicrobial Polypeptides. *Biomacromolecules* **2011,** *12* (5), 1666-1674.
(35) Kenawy el, R.; Worley, S. D.; Broughton, R. The chemistry and applications of antimicrobial polymers: a state-of-the-art review. *Biomacromolecules* **2007,** *8* (5), 1359-1384.
(36) Engler, A. C.; Tan, J. P. K.; Ong, Z. Y.; Coady, D. J.; Ng, V. W. L.; Yang, Y. Y.; Hedrick, J. L. Antimicrobial Polycarbonates: Investigating the Impact of Balancing Charge and Hydrophobicity Using a Same-Centered Polymer Approach. *Biomacromolecules* **2013,** *14* (12), 4331-4339.
(37) Sovadinova, I.; Palermo, E. F.; Huang, R.; Thoma, L. M.; Kuroda, K. Mechanism of polymer-induced hemolysis: nanosized pore formation and osmotic lysis. *Biomacromolecules* **2011,** *12* (1), 260-268.
(38) García-Argüelles, S.; Serrano, M. C.; Gutiérrez, M. C.; Ferrer, M. L.; Yuste, L.; Rojo, F.; del Monte, F. Deep Eutectic Solvent-Assisted Synthesis of Biodegradable Polyesters with Antibacterial Properties. *Langmuir* **2013,** *29* (30), 9525-9534.
(39) Zheng, Z.; Xu, Q.; Guo, J.; Qin, J.; Mao, H.; Wang, B.; Yan, F. Structure-Antibacterial Activity Relationships of Imidazolium-Type Ionic Liquid Monomers, Poly(ionic liquids) and Poly(ionic liquid) Membranes: Effect of Alkyl Chain Length and Cations. *ACS Appl Mater Interfaces* **2016,** *8* (20), 12684-12692.
(40) Zhang, J.; Xiao, Y.; Luo, X.; Wen, L.; Heise, A.; Lang, M. Schizophrenic poly(ε-caprolactone)s: synthesis, self-assembly and fluorescent decoration. *Polym. Chem.* **2017,** *8* (21), 3261-3270.
(41) Zhang, J.; Xiao, Y.; Xu, H.; Zhou, C.; Lang, M. D. Synthesis of well-defined carboxyl poly (ε-caprolactone) by fine-tuning the protection group. *Polym Chem* **2016,** *7* (28), 4630-4637.
(42) M. L, F.; Scandola, M.; Kumar, A.; R. A, G. Physical Characterization of Poly(ω-pentadecalactone) Synthesized by Lipase-Catalyzed Ring-Opening Polymerization. *J Polym Sci Poly Phys* **2001,** *39* (15), 1721-1729.
(43) Yan, J.; Zhang, Y.; Xiao, Y.; Zhang, Y.; Lang, M. Novel poly(ε-caprolactone)s bearing amino groups: Synthesis, characterization and biotinylation. *React Fun Polym* **2010,** *70* (7), 400-407.

(44) Wilson, J. A.; Hopkins, S. A.; Wright, P. M.; Dove, A. P. Synthesis of ω-Pentadecalactone Copolymers with Independently Tunable Thermal and Degradation Behavior. *Macromolecules* **2015,** *48* (4), 950-958.
(45) Liu, R.; Chen, X.; Chakraborty, S.; Lemke, J. J.; Hayouka, Z.; Chow, C.; Welch, R. A.; Weisblum, B.; Masters, K. S.; Gellman, S. H. Tuning the Biological Activity Profile of Antibacterial Polymers via Subunit Substitution Pattern. *J Am Chem Soc* **2014,** *136* (11), 4410-4418.
(46) Luo, L.; Li, G.; Luan, D.; Yuan, Q.; Wei, Y.; Wang, X. Antibacterial adhesion of borneol-based polymer via surface chiral stereochemistry. *ACS Appl Mater Interfaces* **2014,** *6* (21), 19371-19377.
(47) van der Meulen, I.; de Geus, M.; Antheunis, H.; Deumens, R.; Joosten, E. A. J.; Koning, C. E.; Heise, A. Polymers from Functional Macrolactones as Potential Biomaterials: Enzymatic Ring Opening Polymerization, Biodegradation, and Biocompatibility. *Biomacromolecules* **2008,** *9* (12), 3404-3410.

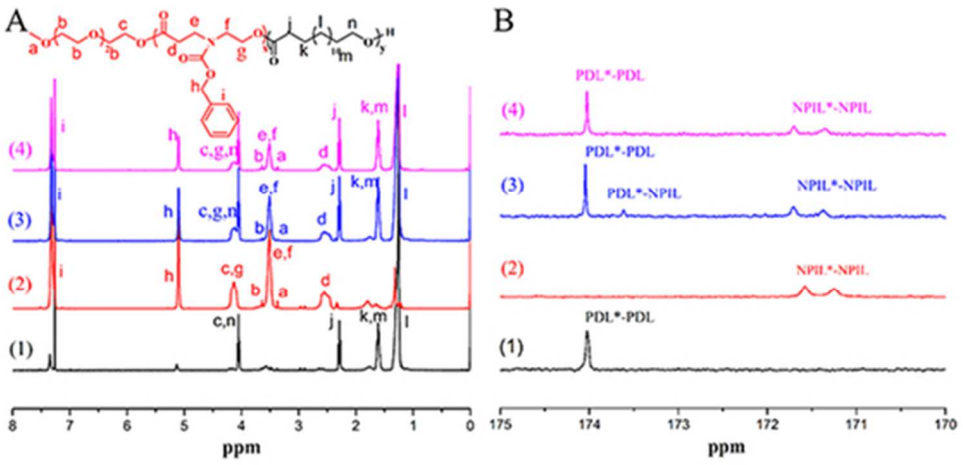

Figure 1. (A) 1H NMR and (B) 13C NMR spectra of products with catalytic systems of (1) Novozym 435; (2) Sn(Oct)2; (3) Novozym 435 and Sn(Oct)2; (4) Sn(Oct)2 then Novozym 435.

49x24mm (300 x 300 DPI)

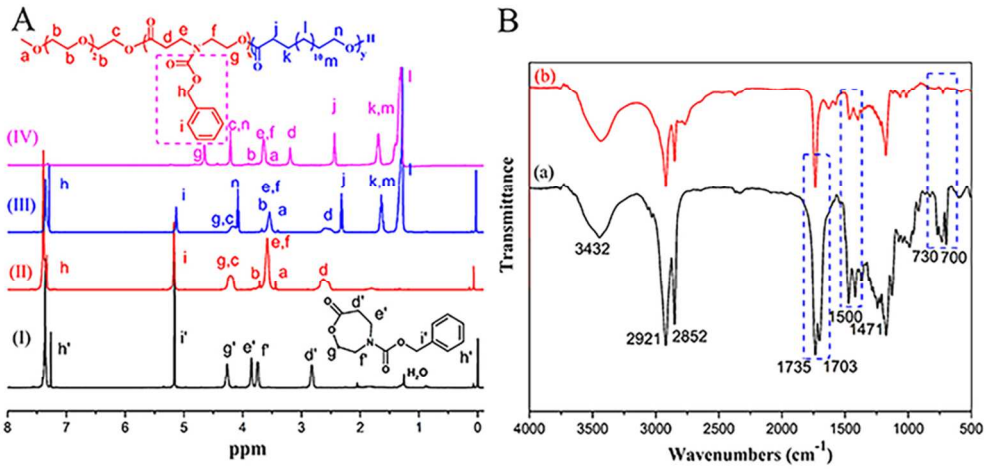

Figure 2 (A) 1H NMR spectra of (I) NPIL, (II) PNPIL50, (III) PNPIL50-b-PPDL50 and (IV) PPIL50-b-PPDL50. (B) FTIR spectra of (a) PNPIL50-b-PPDL50 and (b) PPIL50-b-PPDL50.

81x38mm (300 x 300 DPI)

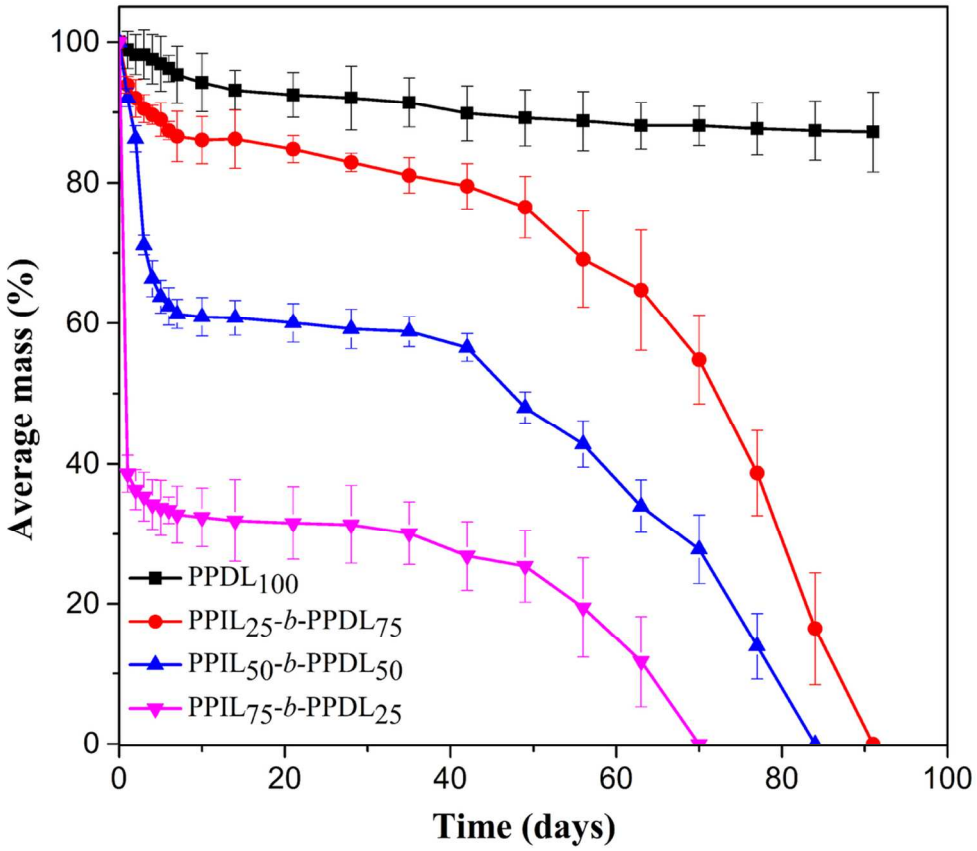

Figure 3. Average mass (%) of PPDL copolymer and homopolymer studied in accelerated degradation conditions (5 M NaOH, 37 oC).

102x87mm (300 x 300 DPI)

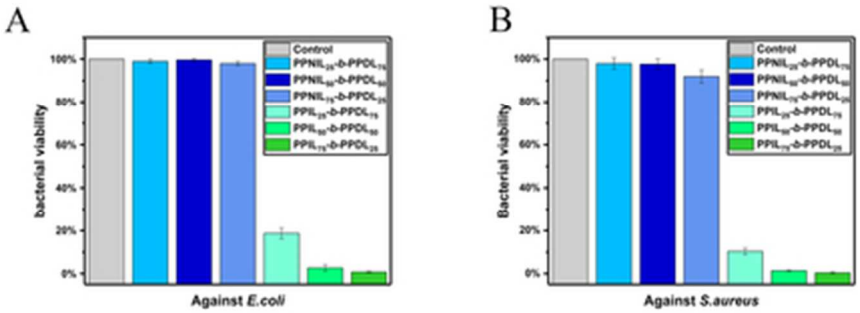

Figure 4. Bacterial viabilities of (A) E. coli and (B) S. aureus after 3 h contacting with PNPIL-b-PPDL and PPIL-b-PPDL copolymers.

37x13mm (300 x 300 DPI)

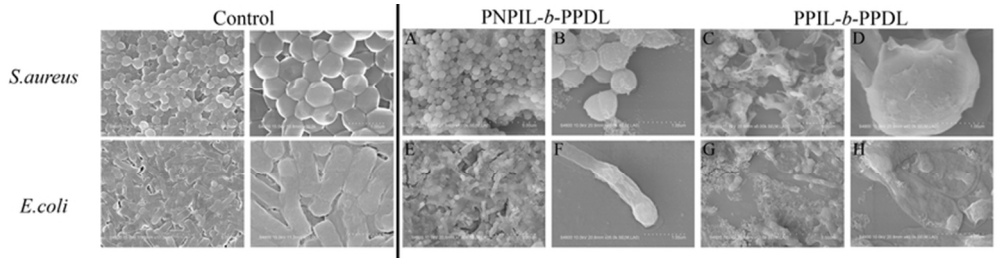

Figure 5. SEM images of S. aureus and E. coil cultured on block copolymers surfaces for 3 h. (left part: healthy bacterial morphologies, mid and right: B, D, F and H are expanded images of A, C, E and G, respectively).

71x18mm (300 x 300 DPI)

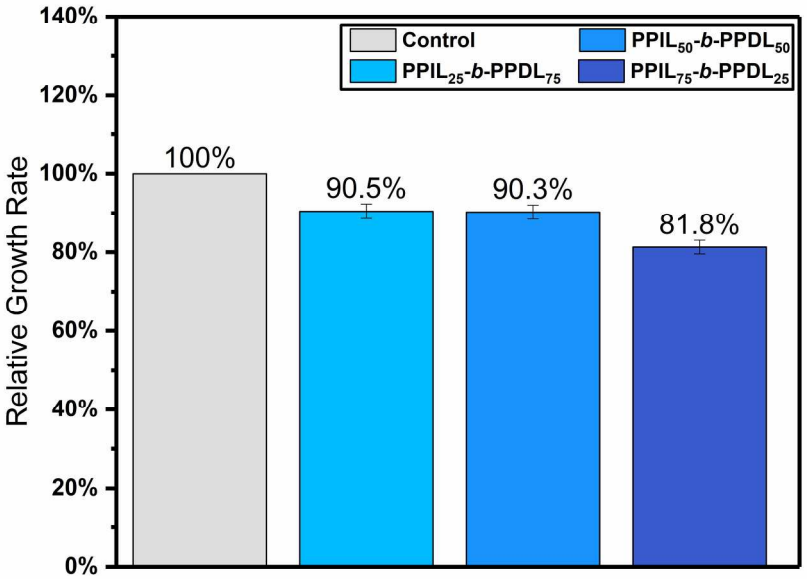

Figure 6. Relative growth rate (RGR) of various PPIL contents membranes to mouse embryonic fibroblast cells detected by MTT assay

208x159mm (300 x 300 DPI)

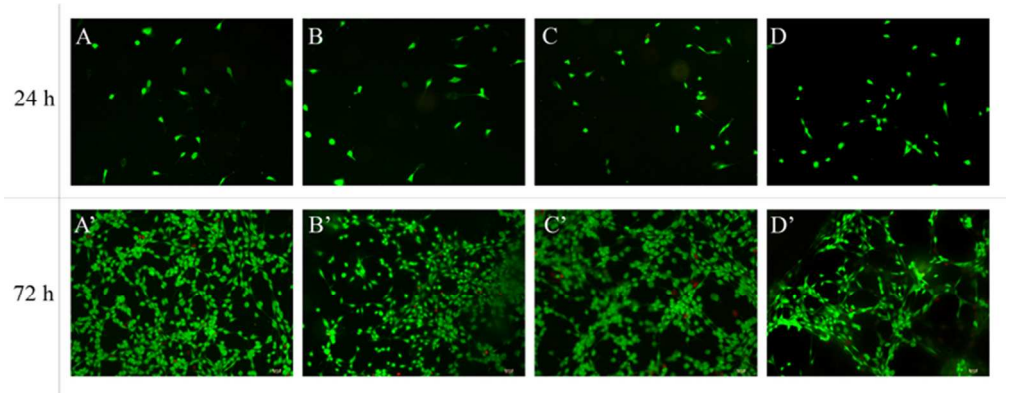

Figure 7. Fluorescence microscopy images (10× magnification) of NIH-3T3 mouse embryonic fibroblast cells after 24 h on CDA (A), PPIL25-b-PPDL75 (B), PPIL50-b-PPDL50 (C), PPIL75-b-PPDL25 (D) surfaces. After 72 h on CDA (A'), PPIL25-b-PPDL75 (B'), PPIL50-b-PPDL50 (C'), PPIL75-b-PPDL25 (D') surfaces after live-dead staining. Green indicates viable cells, and red indicates dead cells.

70x27mm (300 x 300 DPI)

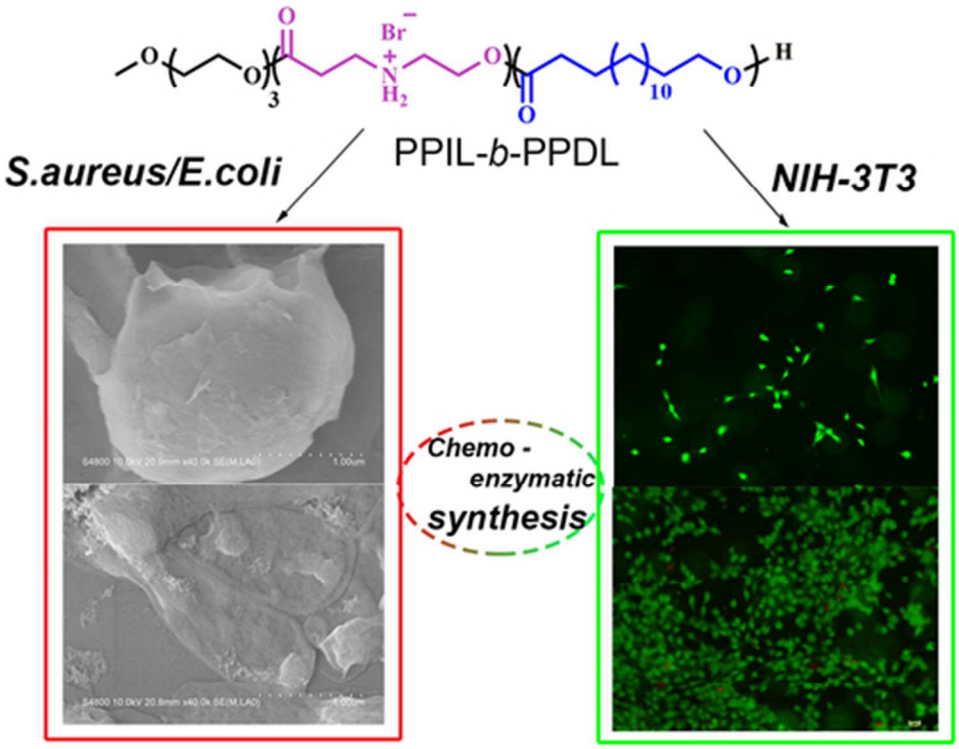

44x35mm (300 x 300 DPI)